Chemical Engineering Journal 152 (2009) 103–109

Contents lists available at ScienceDirect

Chemical Engineering Journal

journal homepage: www.elsevier.com/locate/cej

Riboflavin-sensitized photooxidation of phenylurea herbicide monuron in aqueous peroxide solution

K.H. Chan, W. Chu*

Department of Civil and Structural Engineering, The Hong Kong Polytechnic University, Hunghom, Kowloon, Hong Kong

ARTICLE INFO

Article history:
Received 18 March 2008
Received in revised form 18 March 2009
Accepted 22 March 2009

Keywords:
Monuron
Riboflavin
Photosensitization
Photooxidation
Hydrogen peroxide

ABSTRACT

A natural photosensitizer riboflavin (Rf), known as vitamin B_2, and an environmental friendly strong oxidant hydrogen peroxide (H_2O_2) were employed for the riboflavin-sensitized photooxidation process (UV/Rf/H_2O_2) in this study. This approach could be considered as a hybrid process of UV/Rf (photosensitization) and UV/H_2O_2 (advanced oxidation). The photodecay of a phenylurea herbicide monuron was investigated by varying the doses of Rf and H_2O_2 in this work. The use of UV/Rf/H_2O_2 showed a promising performance for degrading monuron compared with the direct photolysis (UV), UV/Rf, and UV/H_2O_2 processes. It was found that more than 99% of the monuron was removed in the UV/Rf/H_2O_2 process in less than 70 min depending on the dosages of Rf and H_2O_2. In general, the overall improvement of UV/Rf/H_2O_2 process would achieve as high as ~450% comparing to sole-UV process. In addition, a kinetic model for the UV/Rf/H_2O_2 process was developed successfully in this study to facilitate the prediction of the additional performance on the degradation of monuron comparing with the daughter processes (UV, UV/Rf, and UV/H_2O_2).

1. Introduction

Photochemical treatment was an important mechanism for the degradation of environmental pollutants such as pesticides/herbicides. This type of treatment could be optimized by taking into account various factors influencing photoreaction rate, which was proportional to the light absorption rate and to the overall quantum yield (Φ) [1]. The overall quantum yield was the fraction of absorbed light at a wavelength that resulted in the photoreaction of the target compound. However, most of the organic substances did not strongly absorb the light energy or wavelength above 300 nm [2]. Studies showed that through the use of photosensitizers, the degradation of most organic substances at longer UV wavelength (such as UV-B or UV-A) became possible. Photosensitizers absorbed light energy and transformed it into chemical energy during the formation of excited state of molecules and then initiated a series of photochemical reactions for the degradation of the target compound. The process was commonly known as indirect photodegradation which often demonstrated higher quantum efficiency than that of direct photolysis. Some dyes, amines and organic solvents were reported as photosensitizers in treatment processes, such as rose bengal (4,5,6,7-tetrachloro-2′,4′,5′,7′-tetraiodofluorescein) [3], methylene blue [4], diethylamine [5] and acetone [6]. Since their absorption rates at sunlight and near-UV wavelength were generally high, and thus, their excited singlets often performed cross-intersystem to long-lived triplet states that efficiently participate in energy transfer reaction.

Riboflavin (Rf), was a natural pigment present in sensitizing concentrations in water courses, lakes and seas [7]. It has been postulated as a possible sensitizer for the in situ photodegradation of herbicides and other environmental contaminants [8]. Previous studies used Rf-mediated photosensitization (UV/Rf) as the degradation process including mycosporine-like amino acids [3], pesticides 4-hydroxypyridine [9], 2,4,6-trinitrotoluene [8], azo dyes [10], phenol [11], and chlorinated phenols [12].

In this study, an aqueous hydrogen peroxide was introduced to the UV/Rf process in order to further improve the overall performance of the treatment. The aim of these processes was to generate a highly reactive hydroxyl radical ($HO^\bullet$), which would react unselectively with most of the organic and inorganic substances present in water. Chu [13] has concluded that the UV/H_2O_2 process could successfully decayed 2,4-D via the photooxidation mechanisms involving $HO^\bullet$. Thus, in this work, the effects of the doses of Rf and H_2O_2 on the Rf-sensitized photooxidation (i.e., UV/Rf/H_2O_2) would be investigated. Besides, a phenylurea herbicide, monuron, was selected as the target compound in this study. Monuron (3-(4-chlorophenyl)-1,1-dimethylurea; C9H11ClN2O; MW 198.65; MP 170.5–171.5 °C; Sol. 230 mg/L at 25 °C) was widely used as herbicide because of its inhibition of photosynthesis [14]. It was

---

* Corresponding author. Fax: +852 23346389.
E-mail address: cewchu@polyu.edu.hk (W. Chu).

1385-8947/$ – see front matter © 2009 Elsevier B.V. All rights reserved.
doi:10.1016/j.cej.2009.03.038

used mainly for the weed control in non-crop area and as pre-emergence on fruit crops. Its presence in the environment was rather persistent. It was reported that weeks or months were generally required for its decay from environment [15,16]. Besides, the use of monuron was banned recently in some states in US (This information was obtained from South Dakota Department of Agriculture, USA, "Cancelled or Severely Restricted Pesticides in the US").

2. Methodology

2.1. Chemicals

Nonlabeled monuron at 99% purity was purchased from Aldrich Chemical Co. Inc., and Rf at 98% was purchased from International Laboratory USA. Aqueous H_2O_2 (30% solution) were purchased from Junsei Chemical Ltd. (Japan). Sodium azide (NaN_3), and superoxider dismutase (SOD) were from International Laboratory USA and Sigma respectively. Sodium suphate (Na_2SO_3) was purchased from BDH Lab Supplies. Acetonitrile (from Labscan Asia Co. Ltd.) was degassed before being used in liquid chromatography (LC). Sulfuric acid and methanol purchased from Labscan were used to adjust solution pH and prepare quenching solutions, respectively. All chemicals used were HPLC grade and were used as received without further purification. All solutions were prepared by 18 MΩ deionized distilled water from a Bamstead NANOpure water treatment system.

2.2. Method

The stock solution of monuron was prepared at 1.13 mM in distilled-deionized water. The stock solutions of Rf and H_2O_2 in concentrations of 0.11 and 8.8 mM, respectively, were freshly prepared for each experiment and enclosed by aluminum foil to prevent any side reactions from the light in the room. A series of batch tests was employed to determine the degradation of monuron under different concentrations of Rf ([Rf]) and H_2O_2 ($[H_2O_2]$). The tested ranges of [Rf] and $[H_2O_2]$ were 0.00005–0.06 and 0.001–1.323 mM, respectively.

Exact 5 mL reaction solution containing predetermined [Rf], $[H_2O_2]$ and 0.054 mM monuron was prepared and placed in several 15-mL cylindrical quartz cuvettes (with an inner diameter of 13 mm). Since Rf was sensitive to pH ($pK_{a1} = 1.7$, $pK_{a2} = 10.2$ [17]) and its redox potentials were pH dependent [18], the pH level of the experiments was set at pH 5 to avoid the intramolecular proton-association/dissociation, photoreduction and subsequent oxidation of ribityl side-chain [19]. For the photochemical reaction, the sample cuvettes were irradiated in a Rayonet photochemical reactor with sixteen phosphor-coated low-pressure mercury lamps at 300 nm, the cuvettes were placed in a merry-go-round apparatus to ensure an even exposure of the UV. According to the specifications of the photochemical reactor, the photon intensity in the reactor was 1.1×10^{-5} Einstein $L^{-1}\,s^{-1}$. The illuminated samples were removed from the photoreactor at various predetermined reaction time and followed by LC quantification. The LC comprised a Waters 515 HPLC pump, a Waters 717plus Autosampler with a 20 μL injection loop, a Restek pinnacle octyl amine (5 μm, 4.6 mm × 250 mm) column, and a Waters 2487 Dual λ Absorbance Detector. The maximum absorption wavelength of monuron was detected and selected at 244 nm. The mobile phase consisted of 60% acetonitrile and 40% distilled-deionized water was delivered at a flow rate of 1.5 mL min^{-1}, which resulted in a monuron peak at 3.5 min. A 4-point calibration curve was conducted before each batch of experiments to check the accuracy of experiments (where the values of correlation coefficient, R^2, of all calibrations of each batch test were no less than 0.99). All the experiments were conducted in duplicates.

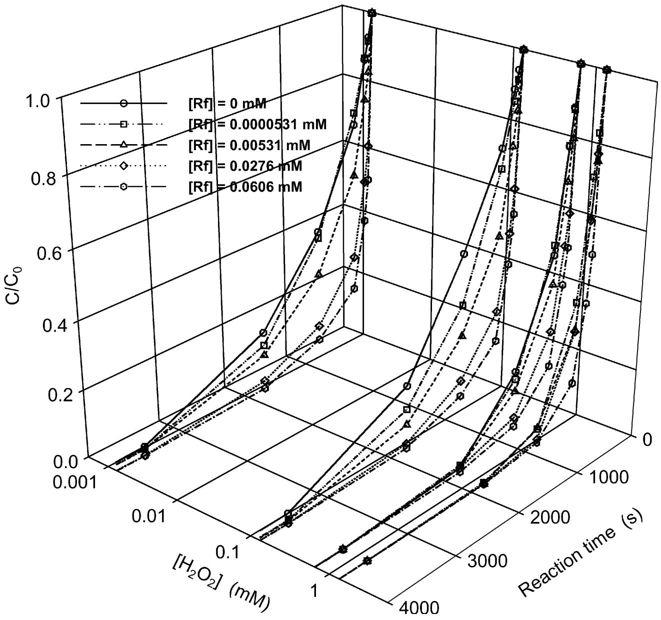

Fig. 1. Degradation of monuron in the UV/Rf/H_2O_2 system with different concentrations of Rf and H_2O_2. (The pseudo first-order rate constants are ranged form 4.47×10^{-3} to $9.40 \times 10^{-4}\,s^{-1}$.)

3. Results and discussion

3.1. Photodecay of monuron by UV/Rf/H_2O_2 process

The decay of monuron by Rf-sensitized photodegradation aided with H_2O_2 was firstly investigated in this work and plotted in Fig. 1. It was found that the decay of monuron would be improved when either the [Rf] or $[H_2O_2]$ was increased. For the process without H_2O_2 (i.e., UV/Rf only), a complete removal of monuron could be achieved within 30 min to 2 h; on the other hand, for the process without Rf (i.e., UV/H_2O_2 only), a complete removal was observed in 1–3 h; while for the process with sole-UV (i.e., $[H_2O_2] = [Rf] = 0$ mM), more than 3 h were required. Resulting from the electronically energy transfer (sensitization) and production of reactive oxygen species such as singlet molecular oxygen ($^1O_2^*$) and superoxide radical anion $O_2^{\bullet-}$, the removal efficiency of the UV/Rf process was improved (Massad et al. [24]). The Rf acted as a sensitizer which could be promoted to excited states electronically through absorption of UV light. The excited forms could directly react with the monuron (as shown in Eqs. (1) and (3); while the reactive oxygen species $^1O_2^*$ and $O_2^{\bullet-}$ yielded from the molecular oxygen dissolving in the medium were generated during the energy transfer process of the sensitization (Eqs. (2) and (4)), and they could chemically react with the monuron (Eqs. (5) and (6)).

Photon absorption/sensitization/intersystem crossing:

$$\mathrm{Rf} \xrightarrow{h\nu} {}^1\mathrm{Rf}^* \xrightarrow{\mathrm{ISC}} {}^3\mathrm{Rf}^* \tag{1}$$

Formation of excited oxygen species:

$$^3\mathrm{Rf}^* + \mathrm{O_2} \rightarrow \mathrm{Rf} + {}^1\mathrm{O_2}^* \,(\text{or } {}^3\mathrm{O_2}) \tag{2}$$

Formation of superoxide anion:

$$^3\mathrm{Rf}^* + \text{monuron} \rightarrow \mathrm{Rf}^{\bullet-} + \text{monuron}^{\bullet+} \tag{3}$$

$$\mathrm{Rf}^{\bullet-} + {}^3\mathrm{O_2} \rightarrow \mathrm{Rf} + \mathrm{O_2}^{\bullet-} \tag{4}$$

$$\mathrm{O_2}^{\bullet-} + \text{monuron or } (\text{monuron}^{\bullet+}) \rightarrow \text{products} \tag{5}$$

Chemical reactions (oxidation):

$$^1O_2^* + \text{monuron} \rightarrow \text{products} \tag{6}$$

On the other hand, for the UV/H_2O_2 process, the formation of hydroxyl radical ($HO^\bullet$) through the direct photolysis of H_2O_2 was observed when the wavelength of UV is less than 360 nm Eq. (7) [20,21], this would enhance the degradation of monuron Eq. (8).Chemical reaction:

$$H_2O_2 \xrightarrow{h\nu} 2HO^\bullet \tag{7}$$

$$HO^\bullet + \text{monuron} \rightarrow \text{products} \tag{8}$$

Though the removal mechanisms of monuron via UV/Rf and UV/H_2O_2 were different, it was interested to find that monuron decay could be improved by combining these two processes (i.e., UV/Rf/H_2O_2), where an accelerated and complete removal of monuron was observed. Referring to Fig. 1, the higher the doses of Rf and/or H_2O_2, the faster decay and the better removal of monuron were observed. It was found that more than 99% of the monuron was removed in the UV/Rf/H_2O_2 process in less than 70 min depending on the dosages of Rf and H_2O_2. If the pseudo first-order rate constants are applied in this analysis, the rates are ranged form 4.47×10^{-3} to $9.40 \times 10^{-4}\ s^{-1}$. Among the processes, by comparing with sole-UV, UV/Rf/H_2O_2 process was observed the best performance which reduced the reaction time by over 12–79% (on 80% removal of monuron) and improved the removal of monuron by over 7–88% (in 10 min of the reaction time); while for UV/Rf process, the reaction time and the removal of monuron were 5–53% and 3–48%, respectively; for UV/H_2O_2 process, those were 4–50% and 2–44%, respectively.

3.2. A series of quenching tests

In order to realize the mechanism of the additional improvement resulted from the UV/Rf/H_2O_2 process, a series of quenching tests was carried out by using SOD, NaN_3, and Na_2SO_3. Kanofsky [22] and Massad et al. [23] suggested that the $O_2^{\bullet-}$ was a key intermediate in the oxygen redox chemistry. Hence, Rf-sensitized photooxidation mediated by $O_2^{\bullet-}$ has been postulated to account for the remediation of a series of compounds in the environment. In this work, however, it was interested to find that the involvement of a strong oxidative species, hydroxyl radicals ($HO^\bullet$), would result in a different mechanism. The quenching tests of the UV/Rf/H_2O_2 process by using different reagents were compared in Fig. 2. It was observed that monuron decayed rapidly in the UV/Rf/H_2O_2 process and more than 98% has been removed after 1 h. The first quenching tests were carried out by using SOD which was used as a quencher mostly targeted to $O_2^{\bullet-}$ [23]. It was found that the overall removal performance (in terms of decay rate and removal percentage) did not show any significant adverse effect involving SOD at the dosages of 0.5 and 2.5 mg. This suggested that the photooxidation mediated by $O_2^{\bullet-}$ should be a minor pathway for the monuron decay in the UV/Rf/H_2O_2 process. On the other hand, NaN_3 was commonly employed to eliminate the participation of $^1O_2^*$ [7,23] and radicals such as superoxide radicals and hydroxyl radicals [24] in reactions. When 5 mM of NaN_3 was added to the UV/Rf/H_2O_2 process, an observable retardation on the monuron decay could be observed, which was even slower than that in the sole-UV process. This was apparently due to the quenching effect on $^1O_2^*$ and other radicals by NaN_3.In order to compare the quenching effects on each process including UV/Rf/H_2O_2, Fig. 3 shows another series of quenching tests on various processes including UV, UV/H_2O_2, and UV/Rf. It was found that the involvement of NaN_3 could not retard the sole-UV process at all. This suggested that the sole-UV process did not involve any radical-related reactions, where direct photolysis of monuron should be dominant in the process. For the UV/H_2O_2 process, its original performance was better than sole-UV process. However, when NaN_3 was added, the performance was significantly reduced and showed poor performance than that of sole-UV. This was because the NaN_3 could quench hydroxyl radicals generated from the UV/H_2O_2, and thus, the decay of monuron only depended on the direct photolysis by UV. In addition, since part of the photons has been consumed to generate the hydroxyl radicals via the UV/H_2O_2, the UV photons available for direct photolysis were reduced.

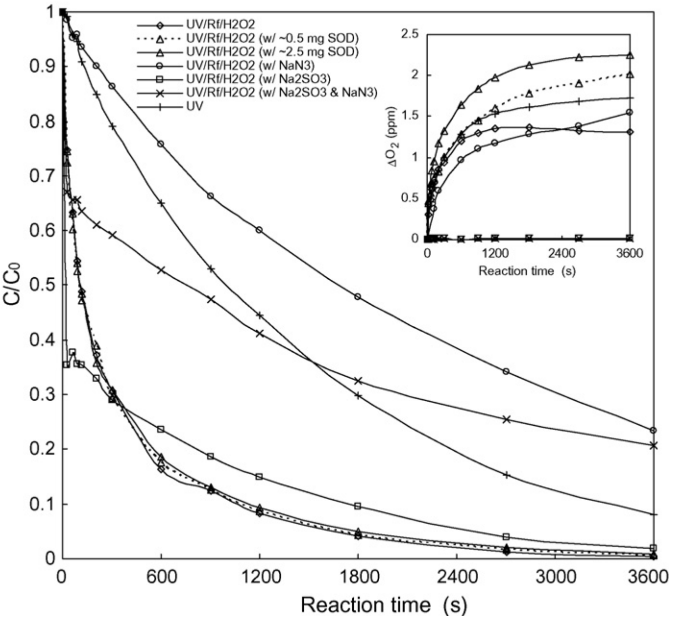

Fig. 2. Quenching tests by using SOD, NaN_3, and Na_2SO_3. The degradation of monuron in different tests (insert: total oxygen consumption in different tests).

On the other hand, similar phenomena were observed in UV/Rf process where the photolysis and sensitized-oxidation (i.e., sensitization together with oxidation) were dominant and resulted in an enhanced degradation of monuron. In the presence of NaN_3, however, the performance of UV/Rf was impeded as the radical-related

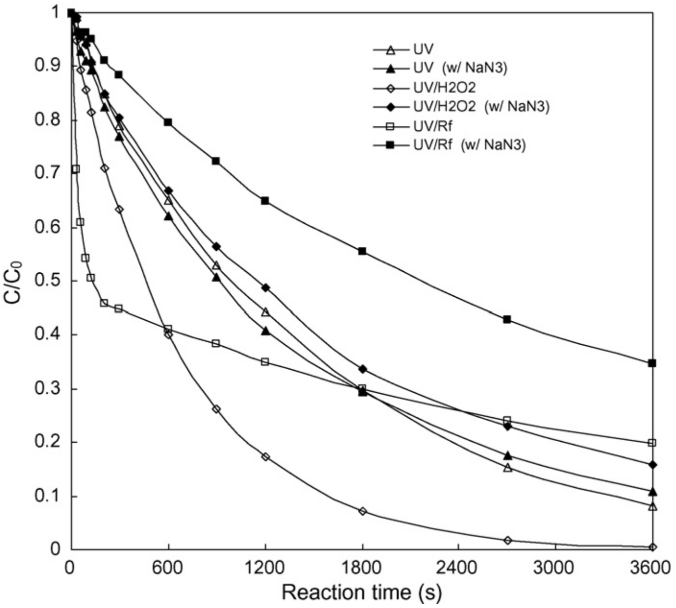

Fig. 3. Degradation of monuron in UV, UV/Rf, and UV/H_2O_2 system with and without the involvement of NaN_3.

reactions and the reactive oxygen species have been quenched. The result showed that the overall performance of UV/Rf process was severely retarded, and it becomes the slowest one among all the tested processes. This could be explained by the observation that the process might be retarded at the later stage (the tailing as show in Fig. 3). This suggested the Rf itself could be decayed upon the UV absorption. The decayed Rf firstly would lose the function of sensitization, then, it became an additional competitor in the solution for the photons, which attenuate the light intensity for monuron decay. Therefore, the faded sensitization and light attenuation resulted in retarding monuron decay, which was observed even slower than that in the sole-UV process as shown in Fig. 2. In additions, Krishna et al. [25] have stated that the reaction involving Rf was implicated in aquatic redox processes. In the presence of triplet molecular oxygen, the process generated reactive oxygenated species such as $^1O_2{}^*$ and $O_2{}^{\bullet-}$ with quantum yields of 0.47 and 0.009, respectively. These reactions could be verified by measuring the oxygen uptake upon photo-irradiation which might attribute to the oxidative species $O_2{}^{\bullet-}$. However, while additional oxidant (e.g., H_2O_2 (or radical) in this study) present in the solution, the reactions involving reactive oxygen species could be masked by the $HO^{\bullet}$-related reactions.

The oxygen consumption of different quenching tests has been also analyzed and plotted as an insert in Fig. 2. However, the overall performance of the process did not show any significant effects due to the oxygen consumption, although the involvement of SOD and NaN_3 could confirm the oxygen uptake in the UV/Rf/H_2O_2 process. For the tests involving SOD, the higher SOD dosage was added, the higher oxygen consumption was observed. However, the reaction with different doses of SOD did not give obvious variation on the overall removal performance. This further verified that the reaction related to $O_2{}^{\bullet-}$ was likely a minor reaction pathway (comparing with hydroxyl radical) in the UV/Rf/H_2O_2 process. While for the tests adding NaN_3, the oxygen uptake was lower initially but the oxygen consumption kept increasing throughout the reaction. This might be due to the fact that the NaN_3 has reacted with the radicals in the reaction such that more dissolved oxygen in the medium has a driving force to continuously convert to reactive oxygen species and react with NaN_3. This resulted in the increasing of oxygen uptake during the reaction by NaN_3, while the overall reaction performance on the degradation of monuron was hindered due to the lack of radicals.

To further verify the importance of the role of oxygen in the process, reducing agent Na_2SO_3 has been added to consume all the dissolved oxygen in the medium before the reaction started. Referring to insert in Fig. 2, it was found that the monuron level dropped significantly in the beginning of the reaction upon the addition of Na_2SO_3. The suddenly drop of the monuron is apparently due to the introduction of a parallel and quick reduction reaction, which reduce monuron together with the original oxidative pathways. Then, the futile interactions between reducing and oxidative agents in the solution would slow down the monuron decay at a later stage. A similar observation was found while adding NaN_3 and Na_2SO_3 to the process, however, the initial drop of the monuron becomes less-significant. This was because the NaN_3 could quench the radicals and attenuate or inhibit the oxidative pathways. Even though, the monuron could continually decay without the radical. This was likely due to the direct photolysis. Finally, extra NaN_3 in the oxygen-free reaction would further retard the reaction. This verified again that other radicals such as $HO^{\bullet}$ existed in the UV/Rf/H_2O_2 process.

3.3. Kinetics analysis on the degradation of monuron in UV/Rf/H_2O_2 process

Since there was an enhancement on the degradation of monuron in the UV/Rf/H_2O_2 process, the photochemical effects of the process were studied by evaluating the observed quantum yields, Φ, under different reaction conditions:

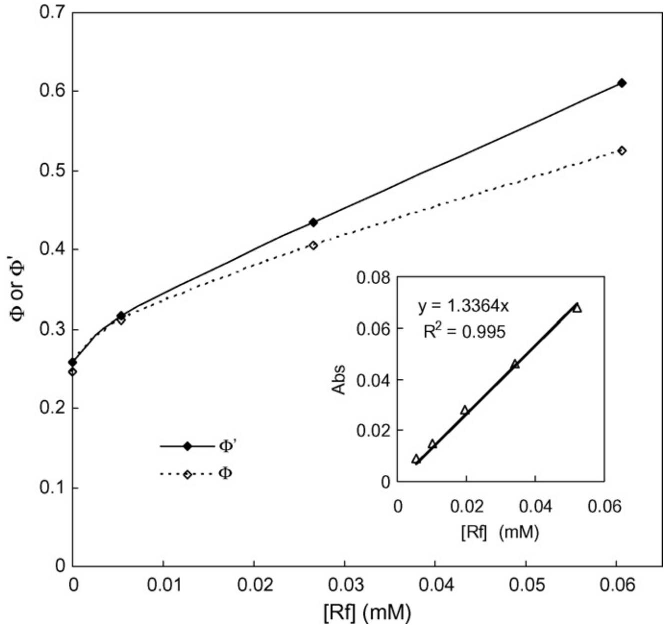

Fig. 4. Corrected quantum yield for the degradation of monuron in the UV/Rf/H_2O_2 system (insert: absorbance of different concentrations of Rf.)

$$\Phi = \frac{k}{2.303 \times I \times \varepsilon \times \ell} \tag{9}$$

where k was the pseudo first-order decay rate constant (s^{-1}) of monuron, I was the light intensity at wavelength 300 nm, ε was the molar absorptivity of monuron at wavelength 300 nm, and ℓ was the cell path length (i.e., 1.3 cm in this study). However, it should be noted that some of the chemicals in the solution were more or less capable of absorbing UV light at 300 nm, which might cause an effect of light attenuation especially if their concentration and/or the associated molar absorptivity was high [26]. The ε of monuron and Rf were measured as 115.9 and 1336.4 L mol^{-1} cm^{-1}, respectively. To evaluate and correct such an effect, Chu et al. [26] have derived an equation to determine the average light intensity, $\bar{I}$ due to absorptions in a tube-type reactor. Thus, the corrected quantum yield, Φ', would be rewritten as,

$$\Phi' = \frac{k}{2.303 \times \bar{I} \times \varepsilon \times \ell} \tag{10}$$

In addition, the Φ' was plotted in Fig. 4 in different [Rf]. It showed that the higher the [Rf], the higher the correction was made. This simply resulted from the attenuation effect due to competitive absorption of Rf. Fig. 5 shows the Φ' in different concentrations of [Rf] and [H_2O_2]. The results were compared with the case of sole-UV (i.e., presented in dashed line in the figure, Φ_{UV}) as well. The points on the y-axis were the cases when no H_2O_2 was involved (i.e., Φ_{Rf} which was the effect due to UV/Rf only), while the points of [Rf] = 0 mM were the Φ' for the UV/H_2O_2 process (i.e., $\Phi_{H_2O_2}$). The figure has presented a full picture of reactions in terms of Φ' with different concentrations of [Rf] and [H_2O_2]. Referring to the figure, the Φ' observed a significant increment even when an extremely small amount of [H_2O_2] was added (0.00132 mM). In additions, the higher the concentrations of [Rf] and/or [H_2O_2] in the process, the higher the Φ'. This observation would then be concluded in Eq. (11), and thus a quantum yield with the additional effect (i.e., Φ_{add}) was defined. Accordingly, the analysis was plotted in Fig. 6 as well:

$$\Phi' = \Phi_{UV} + \Phi_{Rf} + \Phi_{H_2O_2} + \Phi_{add} \tag{11}$$

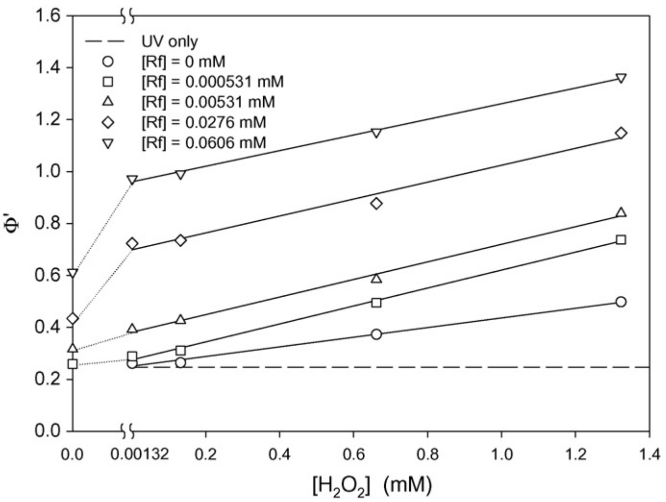

Fig. 5. Corrected quantum yield in different doses of Rf and H_2O_2.

where

$$\Phi_{Rf} = \Phi_{UV/Rf} - \Phi_{UV} \tag{12}$$

and

$$\Phi_{H_2O_2} = \Phi_{UV/H_2O_2} - \Phi_{UV} \tag{13}$$

$$\Phi_{add} = \Phi' - \Phi_{UV} - \Phi_{Rf} - \Phi_{H_2O_2} \tag{14}$$

Mathematically, Φ' was defined as the sum of the performance of sole-UV, UV/Rf and UV/H_2O_2 processes as well as the additional effect besides these processes, Φ_{add}. It should be noted that, Φ_{Rf} and $\Phi_{H_2O_2}$ employed in the equation were defined in Eqs. (12) and (13) respectively, and were excluded the effect due to the sole-UV. Otherwise, the effect due to the sole-UV would be doubling counted in the UV/Rf/H_2O_2 process (i.e., Eq. (11). Thus, to rearrange in Eq. (11), Φ_{add} could be determined. As subtracting the effects due to UV/Rf and UV/H_2O_2 processes (i.e., Φ_{Rf} and $\Phi_{H_2O_2}$, respectively), Φ_{add} would be linearized into a straight line and observed in a positive trend on the increments of Rf and H_2O_2. As shown in Fig. 6, the higher the [Rf] and/or [H_2O_2], the better the Φ_{add} would be resulted. These observations were due to the contributions on UV/Rf which would generate the reactive oxygenated species, and UV/H_2O_2 which would reproduce the stronger oxidizing radicals. The effect was likely due to the very high oxidant (radicals) in the solution, which increased the collision between monuron and oxidant, so the reaction rate (i.e., quantum yield) increased significantly.

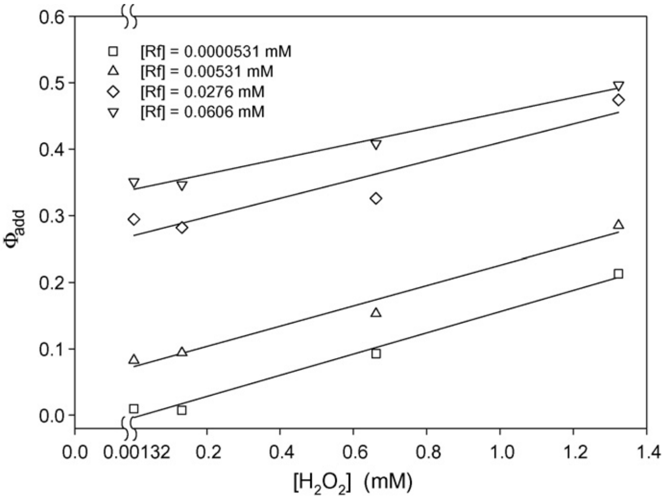

Fig. 6. A plot of Φ_{add} against concentrations of H_2O_2 in different case of [Rf].

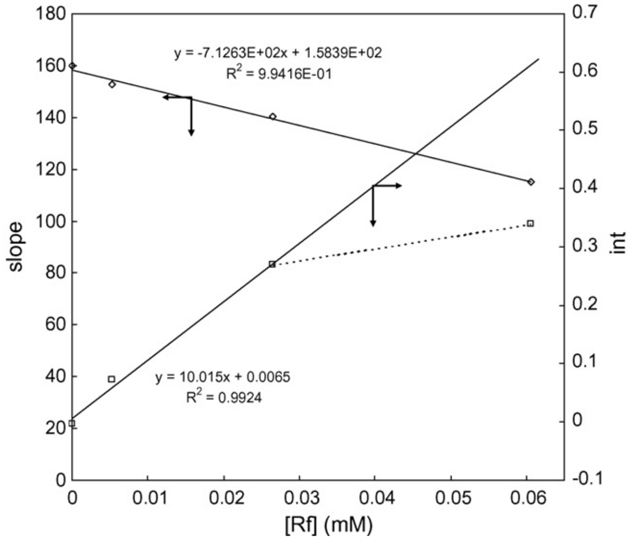

Fig. 7. A plot of $\text{slope}_{\Phi_{add}}$ and $\text{int}_{\Phi_{add}}$ against concentrations of Rf (for the discussion of Eqs. (16) and (17)).

The slopes and intercepts acquired form Fig. 6 could be further analyzed. Depending on the [Rf], the Φ_{add} got a good linear dependence with [H_2O_2] ($\Phi^2 = 0.98–0.99$), and the slopes ($\text{slope}_{\Phi_{add}}$) and intercepts ($\text{int}_{\Phi_{add}}$) of these lines also showed a good correlation in terms of [Rf] (see Fig. 7). Thus, the values of Φ_{add} become predictable, as indicated in Eqs. (15) and (17).

$$\Phi_{add} = \text{slope}_{\Phi_{add}} \times [H_2O_2] + \text{int}_{\Phi_{add}} \tag{15}$$

where

$$\text{slope}_{\Phi_{add}} = -712,630 \times [Rf] + 158.4 \tag{16}$$

$$\text{int}_{\Phi_{add}} = 10,015 \times [Rf] + 0.0065 \tag{17}$$

Referring to Figs. 6 and 7 and Eq. (15), a positive $\text{slope}_{\Phi_{add}}$ was always secured, indicating that the additional performance was proportional to both [Rf] and [H_2O_2], simultaneously. Theoretically, if [Rf] further increased to 0.222 mM (where the $\text{slope}_{\Phi_{add}} = 0$, according to Eq. (16)), the additional performance would be no longer existed and the performance would be independent to [H_2O_2] (i.e., a flat line could be predicted in Fig. 6). Therefore, above this critical [Rf] at 0.222 mM, the additional increasing on [H_2O_2] would not improve the overall performance for the process. This suggested that Rf and its association reactions became dominant in the process.

On the other hand, when [H_2O_2] approached to 0 mM (i.e., at $\text{int}_{\Phi_{add}}$), the Φ_{add} showed a linearly relationship with [Rf] lower than 0.0276 mM. Referring to Fig. 7, there was a ceiling of $\text{int}_{\Phi_{add}}$ at around 0.34, this suggested that excess [Rf] would not give an unlimited enhancement on the degradation of monuron in the UV/Rf/H_2O_2 process. Since the higher absorbance resulted from higher [Rf] concentration would severely attenuate the light (e.g., the absorbance of Rf and monuron was 0.046 and 0.008, respectively in our tests). This effect would firstly leave little UV light to monuron for undergoing direct photolysis; and secondly the solution was turned into an optical dense condition and no longer applicable to the previous calculation.

After solving the Φ_{add}, the degradation of monuron could then be determined by incorporating Eq. (10) to pseudo first-order kinet-

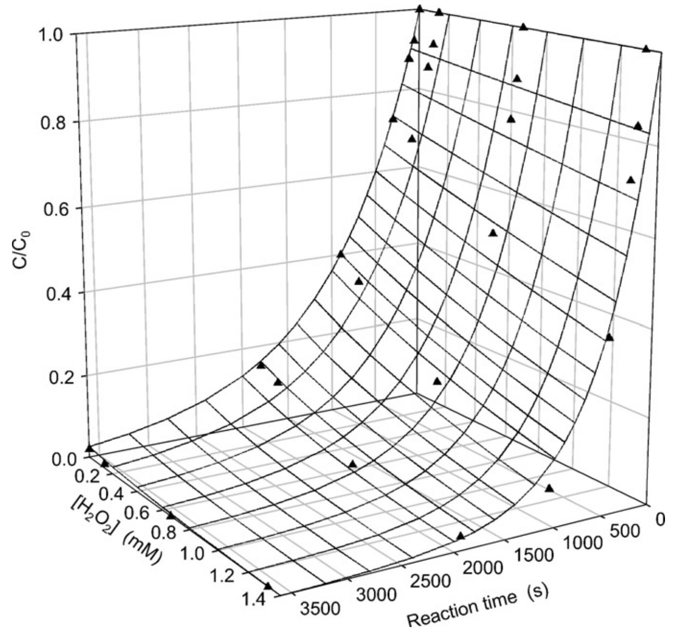

Fig. 8. A typical example on the degradation of monuron in the UV/Rf/H_2O_2 system in which [Rf] = 0.0005 mM. The surface was generated by the proposed modal and the points were the data point for the comparison.

ics, thus,

$$\frac{C}{C_0} = \exp(-2.303 \times \bar{I} \times \varepsilon \times \ell \times \Phi' \times t)$$
$$= \exp(-2.303 \times \bar{I} \times \varepsilon \times \ell \times t \times f([\mathrm{Rf}], [\mathrm{H_2O_2}])) \qquad (18)$$

Hence, the kinetic expression could be established according to the predetermined [Rf] and [H_2O_2] in real applications. A typical example using [Rf] of 0.0005 mM shown in Fig. 8, where the proposed model could properly forecast the decay data in the UV/Rf/H_2O_2 process.

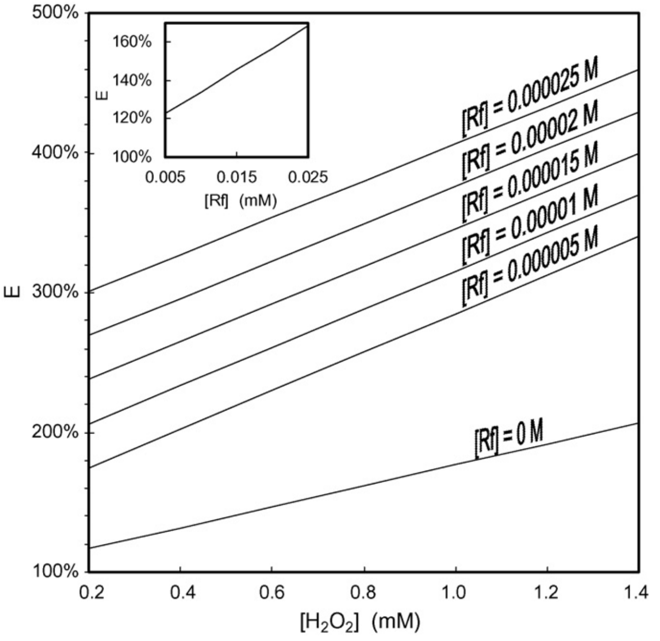

Fig. 9. A diagram plotted for the additional performance resulted from the UV/Rf/H_2O_2 system in different cases of [Rf] (insert: the case in UV/Rf system when no H_2O_2 was involved).

3.4. Reagents dosages analysis

As stated before, the additional enhancement was observed by combining the UV/Rf and UV/H_2O_2 processes. Therefore, an enhancement index, *E*, could be defined as

$$E = \frac{\Phi'}{\Phi_{\mathrm{UV}}} \times 100\% \qquad (19)$$

A diagram illustrating the *E* according to different ranges of [H_2O_2] and [Rf] (where [Rf] $\leq$ 0.025 mM) was generated in Fig. 9a and b. It showed that the higher the [H_2O_2] and/or [Rf], the greater the *E* was obtained, where the magnitude of the additional enhancement has been quantified through the use of *E*. On the other hand, when the [Rf] and [H_2O_2] were selected properly, a better *E* would be guaranteed in the UV/Rf/H_2O_2 process; and the overall improvement would achieve as high as ~450% comparing to sole-UV process.

4. Conclusions

The degradation of monuron by using UV/Rf/H_2O_2, a combination of sensitization (UV/Rf) and advanced oxidation (UV/H_2O_2), has been studied in this work. For UV/Rf process, the sensitization of Rf would generate some reactive oxygenated species which would form ${}^1O_2{}^*$ and $O_2{}^{\bullet -}$ in the process. These species were reported to be the dominant oxidants for the redox reactions in UV/Rf; on the other hand, for UV/H_2O_2 process, in addition to the direct photolysis, a strong oxidizing radical $HO^{\bullet}$ would be generated in the reaction. Both of the processes were found to be able to enhance the direct photolysis process (i.e., sole UV). Moreover, in this study, an additional enhancement could be observed when combining these two processes and resulting in an intensified oxidant level in the solution. This suggested that the use of cocktail approach is possible in real application of water or wastewater treatment. According to our analysis, the maximum/practical Rf dosage is around 0.222 mM; beyond this level, the process becomes H_2O_2 independent. However, it should be noted that the light attenuation and radical competition due to the presence of other organics and suspended solids in the water should be considered. Especially if the proposed model is to be used for prediction purpose, the verification of the model based on the light attenuation and observed rate constants should be conducted for real application or for process scale-up.

Acknowledgment

The work described in this paper was supported by a grant from the University Research Fund of the Hong Kong Polytechnic University (G-U406).

References

[1] R.G. Zepp, in: O. Hutzinger (Ed.), The Handbook of Environmental Chemistry, vol. 2, Springer–Verlag, Berlin, 1982, pp. 19–41, Part B.
[2] J. Hawari, A. Demeter, R. Samson, Sensitized photolysis of polychlorobiphenyls in alkaline 2-propanol: dechlorination of Aroclor 1254 in soil samples by solar radiation, Environ. Sci. Technol. 26 (1992) 2022–2027.
[3] K. Whitehead, J.I. Hedges, Photodegradation and photosensitization of mycosporine-like amino acids, J. Photochem. Photobiol. B: Biol. 80 (2005) 115–121.
[4] A.H. Dwivedi, U.C. Pande, Spectrophotometric study of photosensitized dechlorination of isomeric chloroanisidines, J. Indian Chem. Soc. 82 (2005) 424–427.
[5] Y.J. Lin, G. Gupta, J. Baker, Photodegradation of Aroclor 1254 using diethylamine and simulated sunlight, J. Hazard. Mater. 45 (1996) 259–264.
[6] W. Chu, S.M. Tsui, Modeling of photodecoloration of azo dye in a cocktail photolysis system, Water Res. 36 (2002) 3350–3358.
[7] E. Haggi, S. Bertolotti, N.A. Garcia, Modelling the environmental degradation of water contaminants. Kinetics and mechanism of the riboflavin-sensitised-photo oxidation of phenolic compounds, Chemosphere 55 (2004) 1501–1507.

[8] H. Cui, H.M. Hwang, S. Cook, K. Zeng, Effect of photosensitizer riboflavin on the fate of 2,4,6-trinitrotoluene in a freshwater environment, Chemosphere 44 (2001) 621–625.

[9] A. Pajares, J. Gianotti, G. Stettler, S. Bertolotti, S. Criado, A. Posadaz, F. Amat-Guerri, N.A. Garcia, Modelling the natural photodegradation of water contaminants—a kinetic study on the light-induced aerobic interactions between riboflavin and 4-hydroxypyridine, J. Photochem. Photobiol. A: Chem. 139 (2001) 199–204.

[10] J.A. Field, J. Brady, Riboflavin as a redox mediator accelerating the reduction of the azo dye Mordant Yellow 10 by anaerobic granular sludge, Water Sci. Technol. 48 (2003) 187–193.

[11] R.A. Larson, D.D. Ellis, H.L. Ju, K.A. Marley, Flavin-sensitized photodecomposition of anilines and phenols, Environ. Toxicol. Chem. 8 (1989) 1165–1170.

[12] S. Miskoski, N.A. García, Effect of cholorphenolic pesticides on the photochemistry of riboflavin, Environ. Toxicol. Chem. 25 (1989) 33–43.

[13] W. Chu, Modeling the quantum yields of herbicide 2 4-D decay in UV/H_2O_2 process, Chemosphere 44 (2001) 935–941.

[14] H.C. Bucha, C.V. Todd, 3-(p-Chlorophenyl)-1, 1dimethylurea—a new herbicide, Science 114 (1951) 493–494.

[15] R. White-Stevens, Pesticides in the Environment, Marcel Decker, New York, 1971.

[16] D. Mackay, W.Y. Shiu, K.C. Ma, Illustrated Handbook of Physical–Chemical Properties and Environmental Fate for Organic Chemicals, vol. V, Pesticides Chemicals, Lewis, New York, 1979.

[17] S. Budavari, The Merck Index, 11th ed., Merck & Co. Inc., Rahway, NJ, 1989, pp. 1304–1305.

[18] S.G. Mayhew, The effects of pH and semiquinone formation on the oxidation–reduction potentials of flavin mononucleide—a reappraisal, Eur. J. Biochem. 265 (1999) 698–702.

[19] P.F. Heelis, The photochemistry of flavins, in: F. Muller (Ed.), Chemistry and Biochemistry of Flavoenzymes, vol. 1, CRC Press, Boca Raton, FL, 1991, pp. 171–193.

[20] C. Chevaldonnet, H. Cardy, A. Dargelos, C.I. Abinitio, Calculations on the PE and VUV spectra of hydrogen peroxide, Chem. Phys. 102 (1986) 55–61.

[21] O. Horváth, K.L. Stevenson, Charge-transfer Photochemistry of Coordination Compounds, VCH Publishers, New York, 1993.

[22] J.R. Kanofsky, Singlet oxygen production from the reactions of superoxide ion in aprotic solvents: implications for hydrophobic biochemistry, Free Radical Res. Commun. 12–13 (1991) 87–92.

[23] W. Massad, S. Criado, S. Bertolotti, A. Pajares, J. Gianotti, J.P. Escalada, F. Amat-Guerri, N.A. García, Photodegradation of the herbicide norflurazon sensitized by riboflavin. A kinetic and mechanistic study, Chemosphere 57 (2004) 455–461.

[24] W. Chu, T.K. Lau, S.C. Fung, Effects of combined and sequential addition of dual oxidants (H2O2/S2O82-) on the aqueous carbofuran photodegradation, J. Agric. Food Chem. 54 (2006) 10047–10052.

[25] C.M. Krishna, A. Uppuluri, P. Riesz, J.S. Zigler, D. Balasubramanian, A study on the photolysis efficiencies of some lens constituents, Photochem. Photobiol. 54 (1991) 51–56.

[26] W. Chu, K.H. Chan, C.Y. Kwan, C.T. Jafvert, Acceleration and quenching of the photolysis of PCB in the presence of surfactant and humic materials, Environ. Sci. Technol. 39 (2005) 9211–9216.